IEEE Photonics Journal
An IEEE Photonics Society Publication

Open Access

Polarization Bistability in a 1550 nm Vertical-Cavity Surface-Emitting Laser Subject to Variable Polarization Optical Injection

Volume 9, Number 2, April 2017

Jian-Jun Chen
Zheng-Mao Wu
Li Fan
Xi Tang
Xiao-Dong Lin
Tao Deng
Guang-Qiong Xia

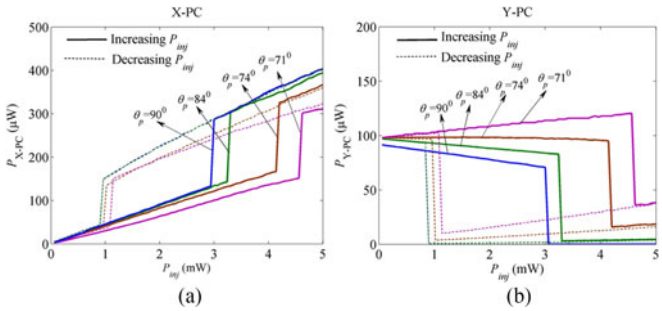

DOI: 10.1109/JPHOT.2017.2690661
1943-0655

Polarization Bistability in a 1550 nm Vertical-Cavity Surface-Emitting Laser Subject to Variable Polarization Optical Injection

Jian-Jun Chen,[1,2] Zheng-Mao Wu,[1] Li Fan,[1] Xi Tang,[1] Xiao-Dong Lin,[1] Tao Deng,[1] and Guang-Qiong Xia[1]

[1]School of Physical Science and Technology, Southwest University, Chongqing 400715, China
[2]School of Medical Engineering and Technology, Xinjiang Medical University, Urumqi 830011, China

DOI:10.1109/JPHOT.2017.2690661

Manuscript received March 14, 2017; revised March 30, 2017; accepted March 31, 2017. Date of publication April 4, 2017; date of current version April 18, 2017. This work was supported in part by the National Natural Science Foundation of China under Grant 61275116, Grant 61475127, Grant 61575163, Grant 61674123, and Grant 61640004; in part by the Natural Science Foundation of Chongqing City under Grant CSTC2016jcyjA0082 and Grant CSTC2016jcyjA0575; and in part by the Fundamental Research Funds for the Central Universities of China under Grant XDJK2014C120 and Grant XDJK2014C079. Corresponding authors: Z.-M. Wu and G.-Q. Xia (e-mail: zmwu@swu.edu.cn; gqxia@swu.edu.cn).

Abstract: The polarization bistability (PB) features in a 1550 nm vertical-cavity surface-emitting laser (1550 nm-VCSEL) subject to variable polarization optical injection (VPOI) are experimentally investigated. We have investigated the influence of polarization angle θ_p of optical injection on PBs induced by scanning the power (power-induced PB) and the frequency of injected light (frequency-induced PB) along with different routes. The experimental results show that, for the fixed frequency of the injection laser and by scanning the injection power within a certain region, there exists a determined range of θ_p in which power-induced PB in the 1550 nm-VCSEL subject to VPOI can be observed. For VPOI with θ_p located within the determined range, the power-induced PB possesses larger hysteresis width, as compared with orthogonally polarized optical injection. The hysteresis width will be larger for a smaller value of θ_p. Under the condition of fixed injection power and continuously varying the frequency of the injection laser, two frequency-induced hysteresis cycles can be observed, of which one is located at negative frequency detuning, and the other is located at positive frequency detuning. The variations of the two hysteresis width with θ_p exhibit different trends. Also, when the bias current of the 1550 nm-VCSEL increases, the hysteresis width can be further broadened for the power-induced PB, and the broadening effect is relatively weak for the frequency-induced PB.

Index Terms: 1550 nm vertical-cavity surface-emitting laser (1550 nm-VCSEL), optical switching device, polarization bistability.

1. Introduction

The phenomenon of optical bistability has attracted much attention due to its wide application prospects in optical information processing, optical flip-flop memory, and optical logic-gate [1]–[5]. Previous studies have demonstrated that the conventional edge-emitting semiconductor lasers

(SLs) can exhibit diverse bistability behavior under external perturbation including optical injection, optical feedback, and optoelectronic feedback. This provides an effective way of performing the bistable operation in all-optical SL systems [6]–[13]. Recently, the bistability in vertical-cavity surface-emitting lasers (VCSELs) has received more focus due its unique advantages such as easy fabrication in two-dimensional arrays, low threshold current, high coupling efficiency with an optical fiber, and reduced manufacturing cost [14]–[16]. In general, the intensity output of a VCSEL is polarized along one of the two orthogonal crystal axes owing to weak material and cavity anisotropies [14]. However, the polarization switching (PS) between the two orthogonal polarization components can be easily triggered by controlling the laser's bias current, operating temperature of the laser [17]–[20], external optical feedback [21]–[24], and external optical injection [25]–[37]. If the switch-on/switch-off points are different and under appropriate scanning of laser's operating parameters, the polarization bistability (PB) with a hysteresis cycle emerges.

External optical injection is an effective way to achieve polarization bistability (PB) in VCSELs. This process of optical injection can be classified as orthogonal optical injection (OOI), parallel optical injection (POI) and variable polarization optical injection (VPOI). In the recent years, there have been extensive investigations on the effects of OOI in VCSELs, where it has shown the PB can be either observed through scanning the injection power (power-induced PB) or the frequency of the injection laser (frequency-induced PB). Based on the spin-flip model (SFM), Sciamanna *et al*. performed a theoretical investigation of characteristics of power-induced and frequency-induced PB in VCSELs subject to OOI [25], [26]. Zhang *et al*. studied the influence of time-varying orthogonal optical injection on hysteresis width of power-induced and frequency-induced PB in VCSELs [28]. Hurtado *et al.* experimentally demonstrated that there exist three different shapes of hysteresis cycle for power-induced PB, and a very wide hysteresis cycle can be observed for frequency-induced PB in a single transverse-mode VCSELs [27], [29]. Torre *et al*. investigated the characteristics of power-induced and frequency-induced PB in VCSELs subject to OOI, and a good overall qualitative agreement has been found between the experimental and theoretical results if the typical values of the VCSELs are considered [30], [32], [36]. Also, PBs in multi-transverse mode VCSELs under OOI had been demonstrated [33], [34]. For the case of POI, the frequency-induced PB behaviors were experimentally observed by Quirce *et al*. in a multi- transverse mode 1550 nm-VCSEL subject to POI [31]. Recently, Guo *et al*. experimentally reported the PB in a single transverse-mode 1550 nm-VCSEL, where an ultra-wide hysteresis cycle of 473.3 GHz for frequency-induced PB and a hysteresis cycle of 7.3 dB for power-induced PB have been experimentally achieved [35].

VPOI is relatively flexible since the polarization angle (θ_p) of optical injection can be easily adjusted. In recent years, the nonlinear dynamics and the polarization evolution in VCSELs under VPOI have received increased interest [38], [39]. In this work, to further understand the PB characteristics of the VCSEL under VPOI, we have performed an experimental investigation on the PB properties of a 1550 nm-VCSEL subject to VPOI. The influences of θ_p on the power-induced and frequency-induced PBs have been extensively studied.

2. Experimental Setup

The schematic of our experimental setup is shown in Fig. 1. A commercial 1550 nm-VCSEL (Raycan) is used in this experiment. The bias current and temperature of the VCSEL are controlled by a high accuracy and low noise current-temperature controller (ILX-Lightwave, LDC-3724C), and the accuracies of bias current and temperature are respectively 0.01 mA and 0.01 °C. Throughout the experiment, the temperature of the VCSEL is stabilized at 20.17 °C. The light emitted from a tunable laser (TL, Santec, TSL-710) passes through a variable attenuator (VA), a polarization controller (PC1), a three-port optical circulator (OC), a 10/90 fiber coupler (FC), and then injected into the VCSEL. PC1 is used to adjust the polarization angle of optical injection (θ_p). VA is employed to control the power level of the injected light from the TL, which is detected by a power meter (PM1). The VCSEL output passes through FC, OC, PC2, polarization beam splitter (PBS), and then is divided into two parts output from terminal port 1 (TP1) and terminal port 2 (TP2), respectively. Through adjusting PC2, it can be realized that the output from TP1 only originates from X polarization

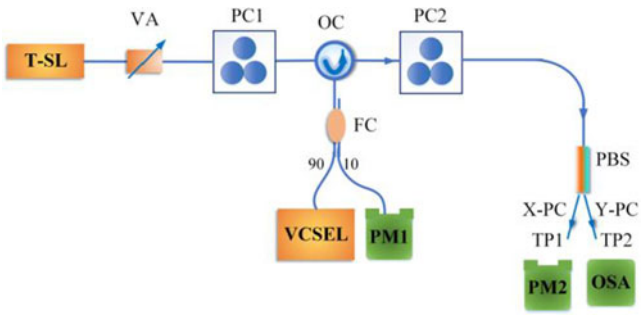

Fig. 1. Schematic diagram of the experimental setup. TL: tunable laser; VA: variable attenuator; PC: polarization controller; OC: optical circulator; FC: fiber coupler; VCSEL: vertical-cavity surface-emitting laser; PBS: polarization beam splitter; TP: terminal port; PM: power meter; OSA: optical spectrum analyzer.

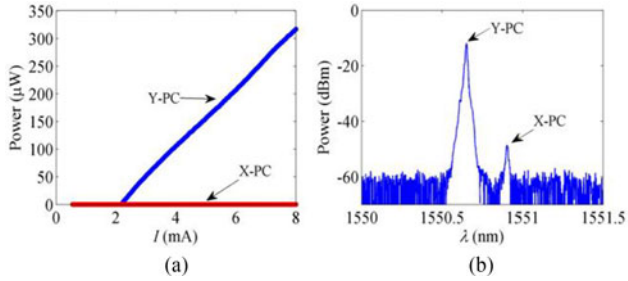

Fig. 2. Experimentally measured (a) polarization-resolved P-I curve and (b) optical spectrum of the stand-alone 1550 nm-VCSEL biased at 5.6 mA.

component (X-PC) of VCSEL, and meanwhile, only Y polarization component (Y-PC) of VCSEL is devoted to the output of TP2. X-PC and Y-PC are sent to a detection system composed of another power meter (PM2) and an optical spectrum analyzer (OSA, Ando AQ6317C, 0.015 nm resolution).

3. Experimental Results and Discussion

Fig. 2(a) represents the experimentally measured polarization-resolved P-I curve of the free-running 1550 nm-VCSEL. It is obvious that, the threshold current of the VCSEL is approximately $I_{th} = 2.20$ mA. For $I_{\text{th}} \leq I < 8.0$ mA, the Y-PC with a short wavelength is always lasing whereas the X-PC with a long wavelength is suppressed. Fig. 2(b) shows the corresponding optical spectrum of the 1550 nm-VCSEL biased at 5.6 mA ($I \approx 2.55\, I_{th}$). The dominant Y-PC oscillates at 1550.65 nm and the subsidiary attenuated X-PC is located at 1550.91 nm, which appears a wavelength (frequency) span of approximate 0.26 nm (32.5 GHz) between the two polarization components. Our experiments further show that for the free-running 1550 nm-VCSEL, only Y-PC of the fundamental transverse mode dominantly oscillates and high-order transverse modes have not be observed within the bias current range of [0 mA, 8 mA].

In the experiment, the polarization direction of the injection light can be varied by controlling PC1. As represented in the Fig. 3(a), E_x and E_y are the slowly varying complex amplitudes of X-PC and Y-PC in the VCSEL respectively. The injected optical field E_{inj} is linearly polarized in a certain direction and can be orthogonally decomposed in the X-PC and Y-PC directions of the VCSEL with amplitudes of E_{injx} and E_{injy}, respectively. Under variable polarization optical injection (VPOI), the polarization angle θ_p of optical injection is defined as the angle between the injected optical field and Y-PC optical field of the VCSEL [39]. Correspondingly, lights injected into the X-PC and Y-PC of the VCSEL are $E_{injx} = E_{inj}\sin\theta_p$ and $E_{injy} = E_{inj}\cos\theta_p$, respectively. The value of θ_p is

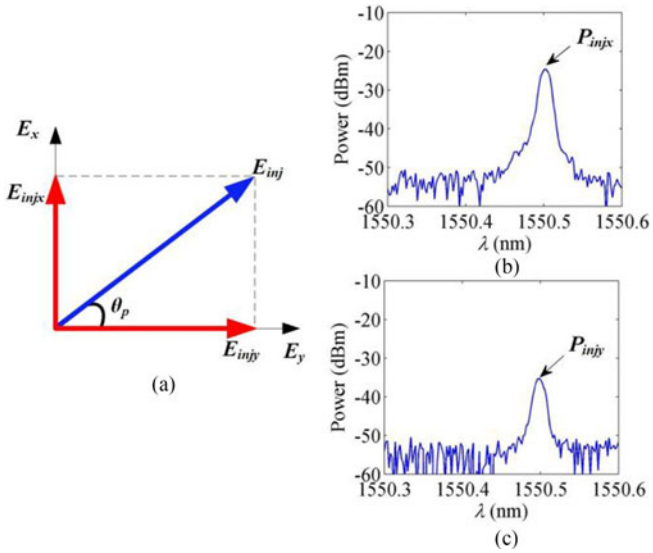

Fig. 3. (a) Diagram of the two orthogonal polarized components of the injected light and the internal optical field in VCSEL. (b) and (c) correspond to optical spectra of the two orthogonal polarized components of the injected light, respectively.

within the range of $0-90^\circ$, where $\theta_p = 0$ and $\theta_p = 90^\circ$ correspond to the case of parallel optical injection (POI) and orthogonally optical injection (OOI) respectively. Fig. 3(b) and (c) demonstrate the spectra of the orthogonal and parallel components of the injected optical field with an arbitrary θ_p, respectively. During the experiment, the measurement of the injected power into X-PC and Y-PC of the VCSEL are as follows: As mentioned above, through adjusting PC2, it can be realized that the outputs of TP1 and TP2 correspond to the X-PC and Y-PC in the VCSEL under no optical injection, respectively. Under this condition, if the bias current is cut off and external optical injection is introduced, the reflected injection light by the front surface of the VCSEL will be entered into PC2 and PBS, and then is output from TP1 and TP2, respectively. Obviously, the output powers from TP1 and TP2 characterize the injection powers into X-PC ($P_{injx} = |E_{injx}|^2$) and Y-PC ($P_{injy} = |E_{injy}|^2$), respectively. Correspondingly, the value of θ_p with respect to arbitrary polarized optical injection can be determined in terms of the trigonometric function relation ($\theta_p = \arctan(\sqrt{P_{injx}}/\sqrt{P_{injy}})$).

Initially, we have concerned on the power-induced PB characteristics of the 1550 nm-VCSEL subject to VPOI through scanning the power P_{inj} of the injection light. Here, the frequency detuning $\Delta\nu$ is defined as the frequency difference between the injected light frequency ν_{inj} and the X-PC frequency of the 1550 nm-VCSEL, and the detuning can be controlled by adjusting the frequency of injected light ν_{inj}. Fig. 4 shows polarization-resolved output powers of (a) X-PC and (b) Y-PC of the 1550 nm-VCSEL biased at $I = 5.6$ mA subject to VPOI with $\Delta\nu = -12.5$ GHz for different θ_p. The injection power P_{inj} is adjusted manually with a step of 0.1 mW along different routes. As shown in this diagram, we first increased P_{inj} from 0 mW to 5 mW and then decreased to 0 mW. The forward and reverse PSs occur between X-PC and Y-PC. For the forward (reverse) PS, the output of X-PC (Y-PC) is switched from an off-state to an on-state. Meanwhile the output of Y-PC (X-PC) experiences an opposite process. The forward and reverse PSs emerge respectively at two different distinct values of P_{inj}, which leads to the appearance of PB with anticlockwise (clockwise) hysteresis loop for the X-PC (Y-PC). And the interval of two specific P_{inj} is the hysteresis width (ΔP) of the PB. It is also observed from Fig. 4 that, in comparison with OOI ($\theta_p = 90^\circ$), VPOI is more constructive for obtaining PB with larger hysteresis width. The hysteresis width will be larger for the smaller value of θ_p. The reason is that, for VPOI, due to the polarization decomposition, a smaller θ_p will lead to a lower injection power P_{injx} into the X-PC of the VCSEL and a higher injection power P_{injy} into the Y-PC of the VCSEL, and hence, a stronger P_{inj} of injection optical field is required to induce

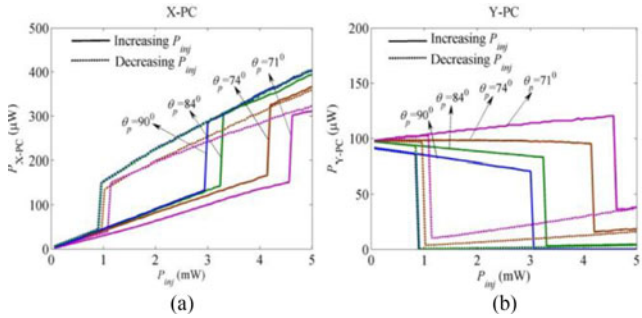

Fig. 4. Polarization-resolved output powers of (a) X-PC and (b) Y-PC in the 1550 nm-VCSEL biased at $I = 5.6$ mA subject to VPOI with $\Delta\nu = -12.5$ GHz and different θ_p, where the solid and dotted lines correspond to the cases of increasing and decreasing P_{inj}, respectively.

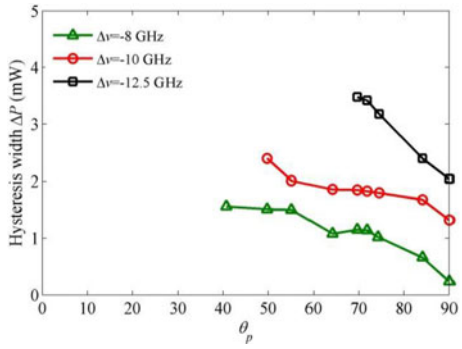

Fig. 5. Variation of ΔP as a function of θ_p under $I = 5.6$ mA and three different values of $\Delta\nu$, where the scanned range of P_{inj} is $0 - 5$ mW.

the power PS for a smaller θ_p. For the mentioned values of θ_p, and its influence on the specific P_{inj} requirement by forward PS is more obvious, which results in the larger hysteresis width compared with that under OOI. It should be pointed out that, for different θ_p the PS strongly depends on the injection power P_{injx} and can be also used to quantize the PB width. The subsequently handling proves the relatively small trend of PB if P_{injx} is considered as the reference. However, from the point of view of increasing the hysteresis width, the larger PB region labelled by the total power P_{inj} can be favored by the PB-based application. Therefore, in the following discussion, P_{inj} is used to characterize the injection condition.

In order to explore the influence of θ_p on the hysteresis width ΔP, the θ_p is varied for three different values of $\Delta\nu$. Fig. 5 depicts the variation of ΔP as a function of θ_p for the 1550 nm-VCSEL biased at 5.6 mA subject to VPOI with $\Delta\nu = -8$ GHz, -10 GHz, and -12.5 GHz, respectively. Under this experimental scenario, P_{inj} is scanned within the range of $0 - 5$ mW, which leads to a threshold value of θ_{p0} existed for observing PS and PB. As shown in the figure, at $\Delta\nu = -8$ GHz, the θ_{p0} is about 41°. And for $\theta_{p0} \leq \theta_p \leq 90°$, a smaller value of θ_p is convenient for achieving PB with a larger ΔP. For a larger $|\Delta\nu|$, the value of θ_{p0} is greater and hysteresis width ΔP is wider. The reason is that, for a larger $|\Delta\nu|$, the nonlinear effect induced by the injection light is weaker, and then a stronger P_{injx} is required for PS and PB. As a result, a larger threshold θ_{p0} is needed due to $\theta_p = \arctan(\sqrt{P_{injx}}/\sqrt{P_{injy}})$.

Fig. 6 shows the variation of ΔP as a function of bias current I with fixed $\Delta\nu = -10$ GHz and $\theta_p = 71°$. It can be seen that ΔP has an increasing tendency as the bias current I increases from 2.8 mA to 8.0 mA, which is similar to the previous results reported in [29]. The broadening of the PB region with the increase of I may be attributed to the dispersive nonlinearity in the VCSEL.

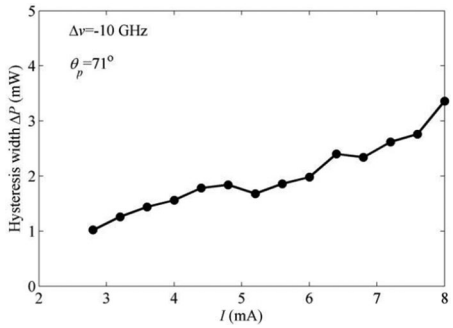

Fig. 6. Variation of ΔP as a function of I under $\Delta\nu = -10$ GHz and $\theta_p = 71^\circ$, where the scanned range of P_{inj} is $0 - 5$ mW.

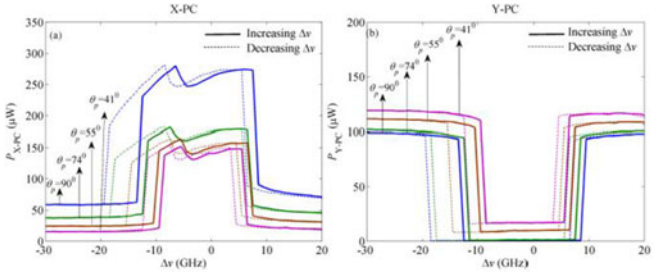

Fig. 7. Polarization-resolved output powers of (a) X-PC and (b) Y-PC of the 1550 nm-VCSEL biased at $I = 5.6$ mA subject to VPOI with $P_{inj} = 2.4$ mW and different θ_p, where the solid and dotted lines correspond to the cases of increasing and decreasing $\Delta\nu$, respectively.

Based on the above experimental results, by adjusting few operational parameters such as θ_p and I, the PB induced by scanning P_{inj} can be controlled effectively to a certain extent.

In addition to the power-induced PB studies, there exists another frequency-induced (or wavelength-induced) PB, which can be realized through scanning ν_{inj} around the suppressed X-PC frequency (ν_x) of the free-running VCSEL [26], [30]. In the following, we have focused on the influence of VPOI on the frequency-induced PB characteristics of the 1550 nm-VCSEL under VPOI. Fig. 7 shows the polarization-resolved output powers of (a) X-PC and (b) Y-PC of the VCSEL biased at $I = 5.6$ mA for different values of θ_p when P_{inj} is fixed at 2.4 mW, and $\Delta\nu$ is scanned along different routes. During the experiment, the frequency detuning $\Delta\nu$ is increased (or decreased) manually with a step of 1 GHz. On one hand, $\Delta\nu$ is increased from –30 GHz to 20 GHz, two successively frequency-induced PSs can be observed, which is located at negative and positive $\Delta\nu$ regions respectively. The PS located at the negative $\Delta\nu$ region occurs when the X-PC of the 1550 nm-VCSEL is locked to the injection light. The PS emerged at the positive $\Delta\nu$ region corresponds to the case that the X-PC is lose-locked to the injection light. On the other hand, for decreasing $\Delta\nu$ from 20 GHz to –30 GHz in a reverse route, two backward PSs can also be observed. The specific values of $\Delta\nu$ required for triggering PSs under forward scanning $\Delta\nu$ are not identical to those under backward scanning $\Delta\nu$, and so two PB regions appears. The width of the hysteresis cycle is defined as the interval of two specific $\Delta\nu$ associated with the forward and backward PSs [36]. Here, the hysteresis cycle located at negative $\Delta\nu$ is named as H1 and the hysteresis cycle located at positive $\Delta\nu$ is named as H2. Similarly, the hysteresis widths are labeled as $\Delta\nu_{H1}$ and $\Delta\nu_{H2}$. From Fig. 7, it can be seen that $\Delta\nu_{H1} = 5$ GHz and $\Delta\nu_{H2} = 2$ GHz for $\theta_p = 90^\circ$. For other values θ_p, the P_{injx} that injected into the X-PC of the VCSEL are lower than the value of $\theta_p = 90^\circ$ due to the decomposition of injection light, that leads to the occurrence of PS at smaller values of $|\Delta\nu|$.

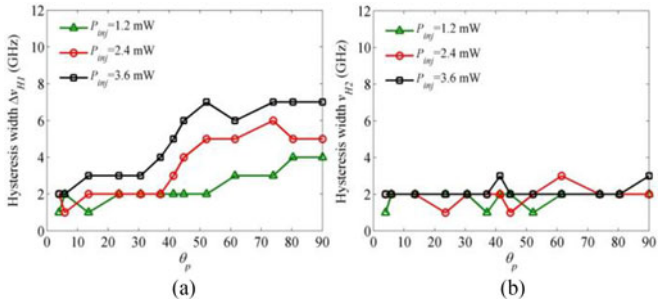

Fig. 8. Variations of $\Delta\nu_{H1}$ (a) and $\Delta\nu_{H2}$ (b) as a function of θ_p for the 1550 nm-VCSEL biased at $I = 5.6$ mA. $\Delta\nu$ is scanned within the range of $-30-20$ GHz.

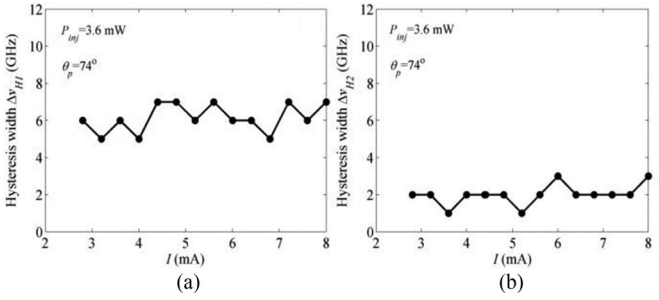

Fig. 9. Variations of $\Delta\nu_{H1}$ (a) and $\Delta\nu_{H2}$ (b) as a function of I with $P_{inj} = 3.6$ mW and $\theta_p = 74^\circ$ when $\Delta\nu$ is scanned within the range of $-30-20$ GHz.

We have further investigated the influence of θ_p on the characteristics of the frequency-induced PB. Fig. 8 represents the measured variations of hysteresis width $\Delta\nu_{H1}$ (a) and $\Delta\nu_{H2}$ (b) as a function of θ_p for the 1550 nm-VCSEL biased at 5.6 mA subject to VPOI with $P_{inj} = 1.2$ mW, 2.4 mW, and 3.6 mW. As shown in the figure, scanning the $\Delta\nu$ within the range of $-30 - 20$ GHz, there exists a threshold value θ_{p0} required for achieving frequency-induced PB, and the θ_{p0} is very small. With an increase of θ_p, the $\Delta\nu_{H1}$ shows a gradual increasing behavior, whereas the $\Delta\nu_{H2}$ almost maintains at a constant variation around 2 GHz.

Correspondingly, the influence of bias current I on the hysteresis width $\Delta\nu_{H1}$ and $\Delta\nu_{H2}$ is carried out and summarized in Fig. 9. It is observed that with an increase of I from 2.8 mA to 8.0 mA, the $\Delta\nu_{H1}$ and $\Delta\nu_{H2}$ exhibits a fluctuation around 6 GHz and 2 GHz respectively. Hence, for frequency-induced PB, in comparison with the results obtained by varying the bias current, we argue that the fine-tuning of θ_p would be relatively more efficient way to control the PB of VCSELs.

By the way, it should be pointed out that during this experimental condition of the 1550 nm-VCSEL biased at 5.6 mA, ultra-wide hysteresis has not been observed for the polarization angle θ_p is near to 90°, and meanwhile irreversible PS mentioned in [36] has not been observed either.

4. Conclusion

In summary, we have experimentally studied the PB characteristics in a 1550 nm-VCSEL subject to variable polarization optical injection (VPOI). We focused our investigation on the influence of polarization angle (θ_p) of optical injection. We have shown that for a fixed frequency detuning ($\Delta\nu$), when the injection power (P_{inj}) is scanned along different routes within a certain range of 0 mW to 5 mW, a power-induced PB can be observed when θ_p locates within a determined region between θ_{p0} (corresponds to the smallest value for the occurrence of PS) and 90°. The value of θ_{p0} is found to be smaller for the small value of $|\Delta\nu|$. For $\theta_{p0} \leq \theta_p \leq 90^\circ$, a smaller θ_p will be more lucrative

to obtain power-induced PB with wider hysteresis width (ΔP). The ΔP can be further extended by increasing the bias current. Next, for scanning $\Delta\nu$ along different routes within a certain range of –30 GHz to 20 GHz, frequency-induced PB, including two successively hysteresis cycles (H1 and H2), can be observed. In comparison with the power-induced PB, the frequency-induced PB can be observed even if the value of θ_p is very small. With an increase of θ_p, the width of the H1 ($\Delta\nu_{H1}$) located at negative $\Delta\nu$ exhibits a gradual increasing trend whereas the width of another hysteresis cycle ($\Delta\nu_{H2}$) located at positive $\Delta\nu$ displays small fluctuations. For a larger P_{inj}, the width of H1 can be further broadened but the width of H2 is almost unchanged. Apart from that, the influence of I on $\Delta\nu_{H1}$ and $\Delta\nu_{H2}$ is not so obvious.

References

[1] H. M. Gibbs, F. A. Hopf, D. L. Kaplan, and R. L. Shoemaker, "Observation of chaos in optical bistability," *Phys. Rev. Lett.*, vol. 46, no. 7, pp. 474–477, Feb. 1981.

[2] F. Ramos *et al.*, "Ist-lasagne: Towards all-optical label swapping employing optical logical gates and optical flip-flops," *J. Lightw. Technol.*, vol. 23, no. 10, pp. 2993–3011, Oct. 2005.

[3] M. Takenaka, K. Takeda, Y. Kanema, Y. Nakano, M. Raburn, and T. Miyahara, "All-optical switching of 40 Gb/s packets by MMI-BLD optical label memory," *Opt. Exp.*, vol. 14, no. 22, pp. 10785–10789, Oct. 2006.

[4] W. D'Oosterlinck *et al.*, "All-Optical flip-flop operation using a SOA and DFB laser diode optical feedback combination," *Opt. Exp.*, vol. 15, no. 10, pp. 6190–6199, May 2007.

[5] K. Huybrechts, G. Morthier, and R. Baets, "Fast all-optical flip-flop based on a single distributed feedback laser diode," *Opt. Exp.*, vol. 16, no. 15, pp. 11405–11410, Jul. 2008.

[6] H. Kawaguchi, I. H. White, M. J. Offside, and J. E. Carroll, "Ultrafast switching in polarization-bistable laser diodes," *Opt. Lett.*, vol. 17, no. 2, pp. 130–132, Jan. 1992.

[7] L. Lin, "Optical frequency bistability and power bistability in semiconductor lasers," *IEEE J. Quantum Electron.*, vol. 31, no. 2, pp. 233–239, Feb. 1995.

[8] L. Lin, "Optical bistability in semiconductor lasers under intermodal light injection," *IEEE J. Quantum Electron.*, vol. 32, no. 2, pp. 248–256, Feb. 1996.

[9] A. Baas, J. P. Karr, H. Eleuch, and E. Giacobino, "Optical bistability in semiconductor microcavities," *Phys. Rev. A*, vol. 69, no. 2, Feb. 2004, Art. no. 023809.

[10] B. Farias, T. P. de Silans, M. Chevrollier, and M. Oria, "Frequency bistability of a semiconductor laser under a frequency-dependent feedback," *Phys. Rev. Lett.*, vol. 94, no. 17, May 2004, Art. no. 173902.

[11] S. Rajesh and V. M. Nandakumaran, "Control of bistability in a directly modulated semiconductor laser using delayed optoelectronic feedback," *Physica D*, vol. 213, no. 1, pp. 113–120, Nov. 2006.

[12] C. Masoller, T. Sorrentino, M. Chevrollier, and M. Oria, "Bistability in semiconductor lasers with polarization-rotated frequency-dependent optical feedback," *IEEE J. Quantum Electron.*, vol. 43, no. 3, pp. 261–268, Mar. 2007.

[13] Y. Y. Xie *et al.*, "Experimental observation of current-induced bistability in a semiconductor laser with positive optoelectronic feedback," *IEEE Photon. Technol. Lett.*, vol. 24, no. 16, pp. 1434–1436, Aug. 2012.

[14] J. Martin-Regalado, F. Prati, M. San Miguel, and N. B. Abraham, "Polarization properties of vertical-cavity surface-emitting lasers," *IEEE J. Quantum Electron.*, vol. 33, no. 5, pp. 765–783, May 1997.

[15] K. Iga, "Surface-emitting laser—Its birth and generation of new optoelectronics field," *IEEE J. Sel. Topics Quantum Electron.*, vol. 6, no. 6, pp. 1201–1215, Nov./Dec. 2000.

[16] F. Koyama, "Recent advances of VCSEL photonics," *J. Lightw. Technol.*, vol. 24, no. 12, pp. 4502–4513, Dec. 2006.

[17] B. Ryvkin *et al.*, "Effect of photon-energy-dependent loss and gain mechanisms on polarization switching in vertical-cavity surface-emitting lasers," *J. Opt. Soc. Amer. B*, vol. 16, no. 11, pp. 2106–2113, Nov. 1999.

[18] Y. Hong *et al.*, "Thermal effects and dynamical hysteresis in the turn-on and turn-off of vertical-cavity surface-emitting lasers," *Opt. Lett.*, vol. 35, no. 21, pp. 3688–3690, Nov. 2010.

[19] M. S. Torre and C. Masoller, "Dynamical hysteresis and thermal effects in vertical-cavity surface-emitting Lasers," *IEEE J. Quantum Electron.*, vol. 46, no. 12, pp. 1788–1794, Dec. 2010.

[20] A. Quirce, A. Valle, L. Pesquera, H. Thienpont, and K. Panajotov, "Measurement of temperature-dependent polarization parameters in long-VCSELs," *IEEE J. Sel. Topics Quantum Electron.*, vol. 21, no. 6, Nov./Dec. 2015, Art. no. 1800207.

[21] Y. Hong, R. Ju, P. S. Spencer, and K. A. Shore, "Investigation of polarization bistability in vertical-cavity surface-emitting lasers subject to optical feedback," *IEEE J. Quantum Electron.*, vol. 41, no. 5, pp. 619–624, May 2005.

[22] Y. Hong, J. Paul, P. S. Spencer, and K. A. Shore, "Influence of low-frequency modulation on polarization switching of VCSELs subject to optical feedback," *IEEE J. Quantum Electron.*, vol. 44, no. 1, pp. 30–35, Jan. 2008.

[23] S. Y. Xiang *et al.*, "Variable-polarization optical feedback induced hysteresis of the polarization switching in vertical-cavity surface-emitting lasers," *J. Opt. Soc. Amer. B*, vol. 427, no. 12, pp. 2512–2517, Dec. 2010.

[24] T. Deng *et al.*, "Impact of optical feedback on current-induced polarization behavior of 1550 nm vertical-cavity surface-emitting lasers," *Appl. Opt.*, vol. 52, no. 16, pp. 3833–3837, May 2013.

[25] M. Sciamanna and K. Panajotov, "Route to polarization switching induced by optical injection in vertical-cavity surface-emitting lasers," *Phys. Rev. A*, vol. 73, no. 2, Feb. 2006, Art. no. 023811.

[26] I. Gatare, K. Panajotov, and M. Sciamanna, "Frequency-induced polarization bistability in vertical-cavity surface-emitting lasers with orthogonal optical injection," *Phys. Rev. A*, vol. 75, no. 2, Feb. 2007, Art. no. 023804.

[27] A. Hurtado, I. D. Henning, and M. J. Adams, "Two-wavelength switching with a 1550 nm VCSEL under single orthogonal optical injection," *IEEE J. Sel. Topics Quantum Electron.*, vol. 14, no. 3, pp. 911–917, May/Jun. 2008.

[28] W. L. Zhang, W. Pan, B. Luo, M. Y. Wang, and X. H. Zou, "Polarization switching and hysteresis of VCSELs with time-varying optical injection," *IEEE J. Sel. Top. Quantum Electron.*, vol. 14, no. 3, pp. 889–894, May/Jun. 2008.
[29] A. Hurtado, A. Quirce, A. Valle, L. Pesquera, and M. J. Adams, "Power and wavelength polarization bistability with very wide hysteresis cycles in a 1550 nm-VCSEL subject to orthogonal optical injection," *Opt. Exp.*, vol. 17, no. 26, pp. 23637–223642, Dec. 2009.
[30] M. S. Torre, A. Quirce, A. Valle, and L. Pesquera, "Wavelength-induced polarization bistability in 1550 nm VCSELs subject to orthogonal optical injection," *J. Opt. Soc. Amer. B*, vol. 27, no. 12, pp. 2542–2548, Dec. 2010.
[31] A. Quirce, A. Valle, A. Hurtado, C. Gimenez, L. Pesquera, and M. J. Adams, "Experimental study of transverse mode selection in VCSELs induced by parallel polarized optical injection," *IEEE J. Quantum Electron.*, vol. 46, no. 4, pp. 467–473, Apr. 2010.
[32] M. S. Torre, A. Hurtado, A. Quirce, A. Valle, L. Pesquera, and M. Adams, "Polarization switching in long-wavelength VCSELs subject to orthogonal optical injection," *IEEE J. Quantum Electron.*, vol. 47, no. 1, pp. 92–99, Jan. 2011.
[33] A. Quirce, J. R. Cuesta, A. Valle, A. Hurtado, L. Pesquera, and M. J. Adams, "Polarization bistability induced by orthogonal optical injection in 1550-nm multimode VCSELs," *IEEE J. Sel. Topics Quantum Electron.*, vol. 18, no. 2, pp. 772–778, Mar./Apr. 2012.
[34] A. A. Qader, Y. Hong, and K. A. Shore, "Ultra-wide hysteresis frequency bistability in vertical cavity surface emitting lasers subject to orthogonal optical injection," *Appl. Phys. Lett.*, vol. 103, no. 2, Jul. 2013, Art. no. 021108.
[35] P. Guo, W. J. Yang, D. Parekh, C. J. Chang-Hasnain, A. S. Xu, and Z. Y. Chen, "Experimental and theoretical study of wide hysteresis cycles in 1550 nm VCSELs under optical injection," *Opt. Exp.*, vol. 21, no. 3, pp. 3125–3132, Feb. 2013.
[36] M. F. Salvide, C. Masoller, and M. S. Torre, "Polarization switching and hysteresis in vertical-cavity surface-emitting lasers subject to orthogonal optical injection," *IEEE J. Quantum Electron.*, vol. 50, no. 10, pp. 848–853, Oct. 2014.
[37] D. Z. Zhong, Y. Q. Ji, and W. Luo, "Controllable optoelectric composite logic gates based on the polarization switching in an optically injected VCSEL," *Opt. Exp.*, vol. 23, no. 23, pp. 29823–29833, Nov. 2015.
[38] A. Hurtado, A. Quirce, A. Valle, L. Pesquera, and M. J. Adams, "Nonlinear dynamics induced by parallel and orthogonal optical injection in 1550 nm vertical-cavity surface-emitting lasers (VCSELs)," *Opt. Exp.*, vol. 18, no. 9, pp. 9423–9428, Apr. 2010.
[39] R. Al-Seyab, K. Schires, A. Hurtado, I. D. Henning, and M. J. Adams, "Dynamics of VCSELs subject to optical injection of arbitrary polarization," *IEEE J. Sel. Topics Quantum Electron.*, vol. 19, no. 4, Jul./Aug. 2013, Art. no. 1700512.